© 2017. Published by The Company of Biologists Ltd | Development (2017) 144, 2730-2736 doi:10.1242/dev.143370

Soluble APP functions as a vascular niche signal that controls adult neural stem cell number

Yuya Sato[1], Yutaka Uchida[1], Jingqiong Hu[1,2], Tracy L. Young-Pearse[3], Takako Niikura[4] and Yoh-suke Mukouyama[1,*]

ABSTRACT

The molecular mechanism by which NSC number is controlled in the neurogenic regions of the adult brain is not fully understood but it has been shown that vascular niche signals regulate neural stem cell (NSC) quiescence and growth. Here, we have uncovered a role for soluble amyloid precursor protein (sAPP) as a vascular niche signal in the subventricular zone (SVZ) of the lateral ventricle of the adult mouse brain. sAPP suppresses NSC growth in culture. Further *in vivo* studies on the role of APP in regulating NSC number in the SVZ clearly demonstrate that endothelial deletion of *App* causes a significant increase in the number of BrdU label-retaining NSCs in the SVZ, whereas NSC/astrocyte deletion of *App* has no detectable effect on the NSC number. Taken together, these results suggest that endothelial APP functions as a vascular niche signal that negatively regulates NSC growth to control the NSC number in the SVZ.

KEY WORDS: APP, Neural stem cell, Subventricular zone, Vascular niche

INTRODUCTION

The vascular niche is now firmly established as a microenvironment that sustains tissue progenitors in close proximity to blood vessels (Rafii et al., 2016). In the neurogenic regions of the adult brain – the subventricular zone (SVZ) of the lateral ventricle and the subgranular zone (SGZ) of the dentate gyrus of the hippocampus (Kriegstein and Alvarez-Buylla, 2009; Ming and Song, 2005; Zhao et al., 2008) – neural stem cells (NSCs) are located in close proximity to specialized capillary endothelial cells (ECs) (Palmer et al., 2000; Shen et al., 2008; Tavazoie et al., 2008). Emerging evidence suggests that these ECs provide signals that direct NSC quiescence and growth (Rafii et al., 2016). In the SVZ, endothelial neurotrophin 3 (NT-3) and ephrin B2 control NSC quiescence as a soluble paracrine and cell-cell contact-dependent signal, respectively (Delgado et al., 2014; Ottone et al., 2014), and endothelial brain-derived neurotrophic factor (BDNF) (Leventhal et al., 1999), pigment epithelium-derived factor (PEDF; also known as Serpinf1) (Ramirez-Castillejo et al., 2006), betacellulin (Gomez-Gaviro et al., 2012) and placental growth factor 2 (PlGF-2) (Crouch et al., 2015) stimulate NSC growth. These studies raise an intriguing question about how multiple vascular signals coordinate NSC quiescence and growth.

Amyloid precursor protein (APP) is widely expressed throughout the adult mouse brain, including in neurogenic regions such as the SVZ (Caille et al., 2004) and SGZ (Guo et al., 2012; Wang et al., 2014), and affects embryonic and adult neurogenesis in mice (Baratchi et al., 2012; Caille et al., 2004; Ma et al., 2008; Wang et al., 2014, 2016). The secreted form of APP (soluble APP, sAPP) has been reported to enhance proliferation of SVZ-NSCs (Baratchi et al., 2012; Caille et al., 2004; Ohsawa et al., 1999) and SGZ-NSCs (Baratchi et al., 2012). Interestingly, infusion of sAPP increased the proliferation of epidermal growth factor (EGF)-responsive neurosphere-forming SVZ-NSCs *in vivo* (Caille et al., 2004), whereas *App* deficiency enhanced the proliferation of neural progenitors in the SGZ (Wang et al., 2014, 2016). Despite the significant roles of APP in adult neurogenesis, the potential involvement of APP as a vascular niche signal in maintaining SVZ-NSCs has not been studied.

In this study, we attempted to identify EC-derived soluble signals that control NSC number in the SVZ. We found that brain microvascular EC line (bEND3)-derived conditioned medium (CM) increased the number of SVZ-derived neurospheres and decreased the size of individual neurospheres in culture. One of the 29 proteins we identified from the bEND3-CM, sAPP, was shown to enhance neurosphere-forming potential but suppress NSC growth in culture. Furthermore, our extensive studies in conventional and cell type-specific mutant mice clearly demonstrate that endothelial APP negatively regulates NSC number in the SVZ.

RESULTS AND DISCUSSION

Brain EC-derived soluble factors enhance neurosphere-forming potential but suppress NSC growth in culture

To improve our understanding of the nature of vascular niche signals for NSC maintenance, we used an established neurosphere culture (passaged neurospheres) from adult mouse SVZ cells (Fig. 1A). Passaged neurospheres were cultured with a medium conditioned by bEND3 cells, which have been reported to support NSCs (Ottone et al., 2014; Shen et al., 2004). We found that the bEND3-CM increased the number of SVZ-derived neurospheres and decreased the size of individual neurospheres (Fig. 1B-E). After cells had been treated with bEND3-CM, secondary neurospheres formed in normal growth medium at a significantly higher number but with a smaller size (Fig. 1F,G), suggesting that the bEND3-CM enhances neurosphere-forming potential but suppresses NSC growth in culture. The bEND3-CM treatment did not affect multipotency of SVZ-NSCs, as differentiation of neurospheres into neurons, astrocytes and oligodendrocytes was observed (Fig. 1H-M). No significant pro-differentiative effects of bEND3-

[1]Laboratory of Stem Cell and Neuro-Vascular Biology, Genetics and Developmental Biology Center, National Heart, Lung, and Blood Institute, National Institutes of Health, Building 10/6C103, 10 Center Drive, Bethesda, MD 20892, USA. [2]Stem Cell Center, Wuhan Union Hospital, Tongji Medical College, Huazhong University of Science and Technology, Wuhan, Hubei 430022, China. [3]Ann Romney Center for Neurologic Diseases, Brigham and Women's Hospital and Harvard Medical School, 77 Avenue Louis Pasteur, Boston, MA 02115, USA. [4]Department of Information and Communication Sciences, Faculty of Science and Technology, Sophia University, 7-1 Kioi-cho, Chiyoda-ku, Tokyo 102-8554, Japan.

*Author for correspondence (mukoyamay@mail.nih.gov)

J.H., 0000-0002-0284-7235; Y.M., 0000-0002-9084-4922

Received 5 August 2016; Accepted 29 June 2017

Development (2017) 144, 2730-2736 doi:10.1242/dev.143370

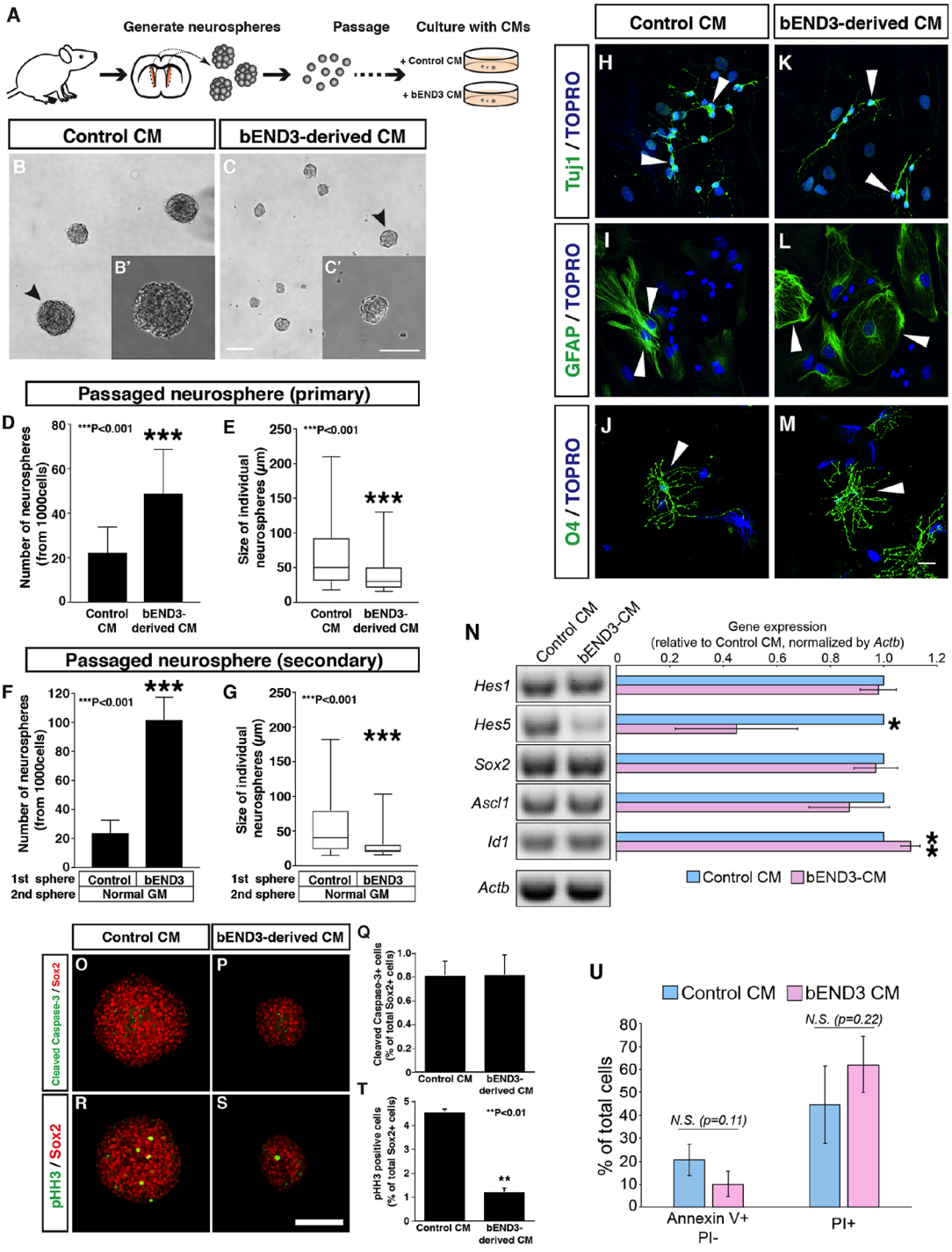

Fig. 1. Brain EC-derived soluble factors influence SVZ-NSC behaviors in culture. (A) Schematic of the experimental design. (B,C) Images of typical passaged neurospheres in the medium containing CM from fresh Opti-MEM (control CM) or bEND3 culture (bEND3-derived CM). Individual neurospheres (arrowheads) are magnified in the insets (B′,C′). (D,E) Quantification of primary neurosphere number (D; *n*=16 wells of 96-well plates from four independent experiments) and size (E; *n*=172 and 348 individual neurospheres in the control and bEND3-CM, respectively, from three independent experiments). (F,G) Quantification of secondary neurosphere number (F; *n*=16 from four independent experiments) and size (G; *n*=256 and 646 in control and bEND3-CM, respectively, from four independent experiments). Individual passaged neurospheres from the culture containing bEND3-CM and control CM were dissociated by trituration, and then re-plated at clonal density in the normal neurosphere growth medium (GM) without any CM. (H-M) Representative images showing the differentiation of passaged neurospheres into Tuj1 (Tubb3)$^{+}$ neurons (H,K, green), GFAP^{+} astrocytes (I,L, green) and O4^{+} oligodendrocytes (J,M, green). Nuclei were stained with TO-PRO-3 (blue). (N) RT-PCR analysis of *Hes1*/*5*, *Sox2*, *Ascl1* and *Id1* expression in passaged neurospheres (left panel). Right panel shows quantification of gene expression relative to *Actb* from three independent experiments. (O,P) Whole-mount neurosphere staining with antibodies to a cell death marker, cleaved caspase-3 (green), together with an NSC marker, Sox2 (red). (Q) Quantification of cleaved caspase-3^{+} dying cells. (R,S) Whole-mount neurosphere staining with antibodies to a proliferation marker, phospho-histone H3 (pHH3, green), and Sox2 (red). (T) Quantification of pHH3^{+} NSCs. (U) Cell viability was assessed by the apoptosis marker Annexin V-Alexa488 and the dead cell marker propidium iodide (PI) after plating for 24 h in the presence of control CM or bEND3-CM. Bars represent mean±s.d. **P*<0.05; ***P*<0.01; ****P*<0.001 (Student's *t*-test). Scale bars: 100 µm (B-C′,O-S); 20 µm (H-M).

Development (2017) 144, 2730-2736 doi:10.1242/dev.143370

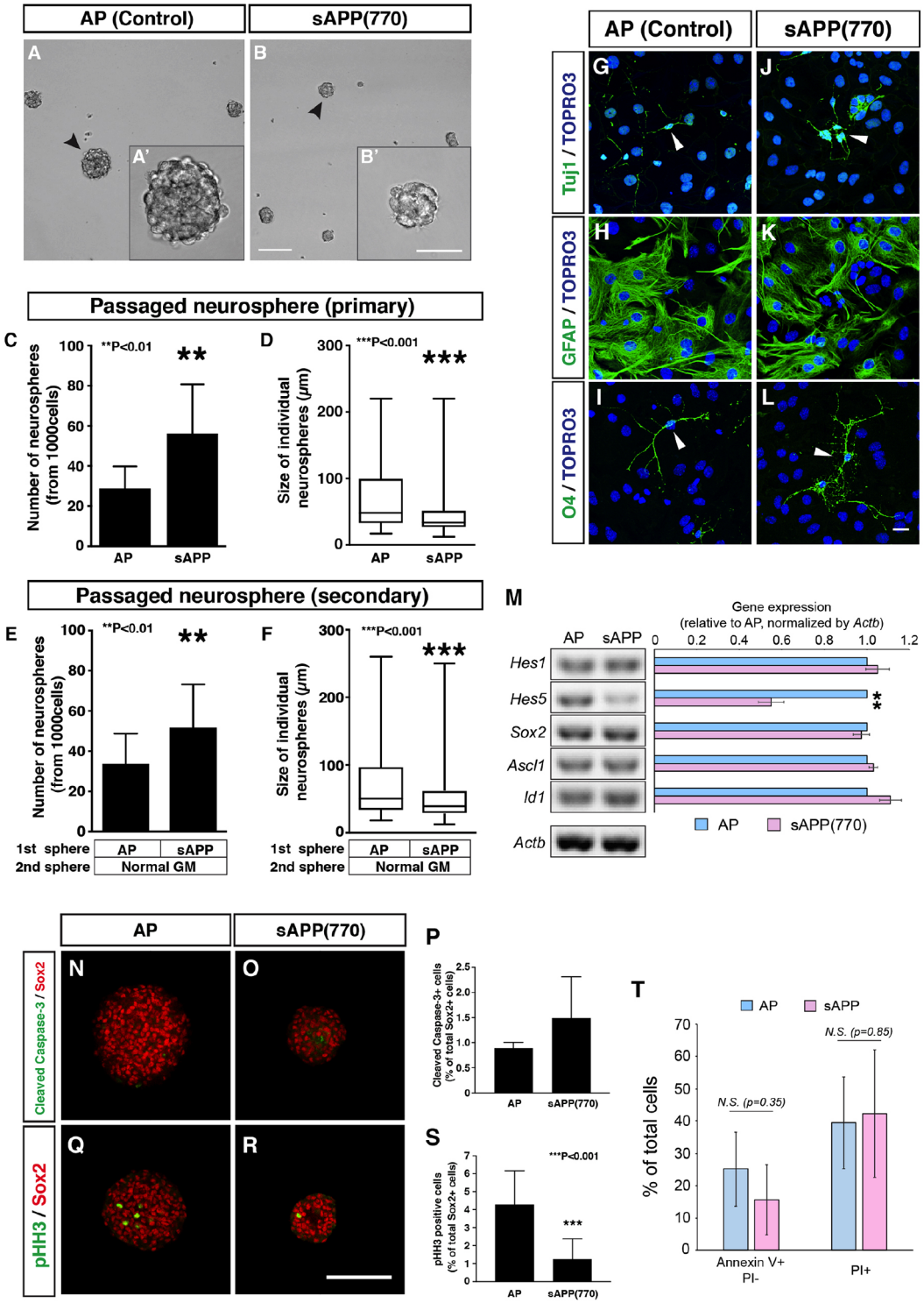

Fig. 2. Soluble APP serves as an EC-derived signal to influence SVZ-NSC behaviors in culture. (A,B) Images of typical passaged neurospheres grown in the presence of control alkaline phosphatase (AP) or sAPP(770). Individual neurospheres (arrowheads) are magnified in the insets (A′,B′). (C,D) Quantification of primary neurosphere number (C; *n*=12 wells of 96-well plates from three independent experiments) and size [D; *n*=166 and 312 individual neurospheres in control AP and sAPP(770), respectively, from three independent experiments]. (E,F) Quantification of secondary neurosphere number (E; *n*=16 from four independent experiments) and size [F; *n*=209 and 294 in control AP and sAPP(770), respectively, from four independent experiments]. (G-L) Representative images showing the differentiation of passaged neurospheres into Tuj1$^+$ neurons (G,J, green), GFAP$^+$ astrocytes (H,K, green) and O4$^+$ oligodendrocytes (I,L, green). Nuclei were stained with TO-PRO-3 (blue). (M) RT-PCR analysis of *Hes1*/*5*, *Sox2*, *Ascl1* and *Id1* expression in passaged neurospheres (left panel). Right panel shows quantification of gene expression relative to *Actb* from three independent experiments. (N,O) Whole-mount neurosphere staining with antibodies to cleaved caspase-3 (green) and Sox2 (red). (P) Quantification of cleaved caspase-3$^+$ dying cells. (Q,R) Whole-mount neurosphere staining with antibodies to pHH3 (green) and Sox2 (red). (S) Quantification of pHH3$^+$ NSCs. (T) Cell viability was assessed by Annexin V-Alexa488 and PI after plating for 24 h in the presence of control AP or sAPP(770). Bars represent mean±s.d. ***P*<0.01; ****P*<0.001 (Student's *t*-test). Scale bars: 100 µm (A,B); 50 µm (A′,B′); 20 µm (G-L); 100 µm (N-R).

Development (2017) 144, 2730-2736 doi:10.1242/dev.143370

CM on NSCs were observed in culture (Fig. S1). We further examined the expression of key transcription factors such as *Hes1/5*, *Sox2*, *Ascl1* (also known as *Mash1*) and *Id1-4*, which are characteristic of NSCs (Jung et al., 2010; Nam and Benezra, 2009; Ramirez-Castillejo et al., 2006). The bEND3-CM did not affect the expression of these genes, apart from a significant reduction of *Hes5* expression and a slight increase of *Id1* expression (Fig. 1N; data not shown), corroborating the observation that the bEND3-CM-treated neurospheres retain NSC features. The effects of the bEND3-CM on the size of individual neurospheres were not due to an increase in cell death (Fig. 1O-Q). Rather, phospho-histone H3$^+$ proliferating cells were significantly decreased in the bEND3-CM-treated Sox2$^+$ NSCs (Fig. 1R-T). The effect of bEND3-CM on the number of neurospheres is unlikely to be due to increased cell viability, because the number of apoptotic and necrotic cells remained unchanged after the bEND3-CM treatment (Fig. 1U). Combined, these results suggest that EC-derived signals enhance neurosphere-forming potential but suppress NSC growth in culture.

sAPP enhances neurosphere-forming potential but suppresses NSC growth in culture

To identify EC-derived soluble factors, the CM proteins were fractionated by heparin-affinity chromatography. Based on the fractions' effects on the number and size of neurospheres, we focused on the fraction eluted by 300 mM NaCl (Fig. S2A). Liquid chromatography-mass spectrometry (LC-MS) analysis of the fraction revealed 29 proteins, some of which were examined for their effects on a neurosphere culture derived from acutely dissociated SVZ cells (Fig. S2B,C). Of these, we focused on sAPP because it was also identified from our secreted molecule profiling of the adult SVZ ECs (Lee et al., 2012). Of note, blocking antibodies against sAPP did not affect the number or the size of neurospheres in the bEND3-CM-containing culture, suggesting that other factor(s) may cooperate with sAPP (Fig. S2D,E).

Among different fragments of sAPP (Caille et al., 2004; Ohsawa et al., 1999; Olsen et al., 2014; Willem et al., 2015), the soluble N-terminal fragment (aa 18-286) and the 770 aa form sAPP(770) negatively regulate NSC growth but do not affect the number of neurospheres in the culture from acutely dissociated SVZ cells (Fig. S3). We further evaluated the effect of sAPP(770) on NSC behaviors in the established neurosphere culture (passaged neurospheres). As seen in the bEND3-CM treatment, sAPP(770) increased the number and decreased the size of both primary (Fig. 2A-D) and secondary (Fig. 2E,F) neurospheres while retaining their multipotency (Fig. 2G-L). These data suggest that sAPP(770) enhances neurosphere-forming potential but suppresses NSC growth in culture. sAPP(770) did not affect the expression of the key transcription factors, except for a significant reduction of *Hes5* expression (Fig. 2M; data not shown). sAPP(770) treatment decreased the number of proliferating cells but did not appear to affect cell death in Sox2$^+$ NSCs (Fig. 2N-S). The number of apoptotic and necrotic cells remained unchanged after sAPP(770) treatment (Fig. 2T). These results are similar to the effects of bEND3-CM on NSCs in culture.

APP negatively regulates the SVZ-NSC number *in vivo* in a non-cell-autonomous manner

Previous studies showed that APP is expressed in the SVZ (Caille et al., 2004). To confirm APP expression by an independent method, we performed RT-PCR experiments on acutely isolated ECs from mouse SVZ and cortex by fluorescence-activated cell sorting (FACS). We detected *App* variants in both SVZ and cortex ECs (Fig. S4), indicating that the SVZ ECs express APP, but its expression is not specific to SVZ ECs.

To investigate whether APP plays a similar role in regulating the NSC number *in vivo*, we performed a label-retention assay using 5-bromodeoxyuridine (BrdU) in the adult SVZ of *App* null mutants (Zheng et al., 1995) and their control littermates. BrdU$^+$ label-retaining cells are defined as SVZ-NSCs because the cells have a relatively long cell-cycle time, co-express Sox2 (Fig. S5A,B) and GFAP (data not shown), but do not express any differentiation markers including S100 (Fig. S5C,D). Consistent with previous studies (Shen et al., 2008; Tavazoie et al., 2008), BrdU$^+$ label-retaining NSCs were localized in close proximity to PECAM1$^+$ capillaries in the SVZ (Fig. 3A). *App* null mutants exhibited a

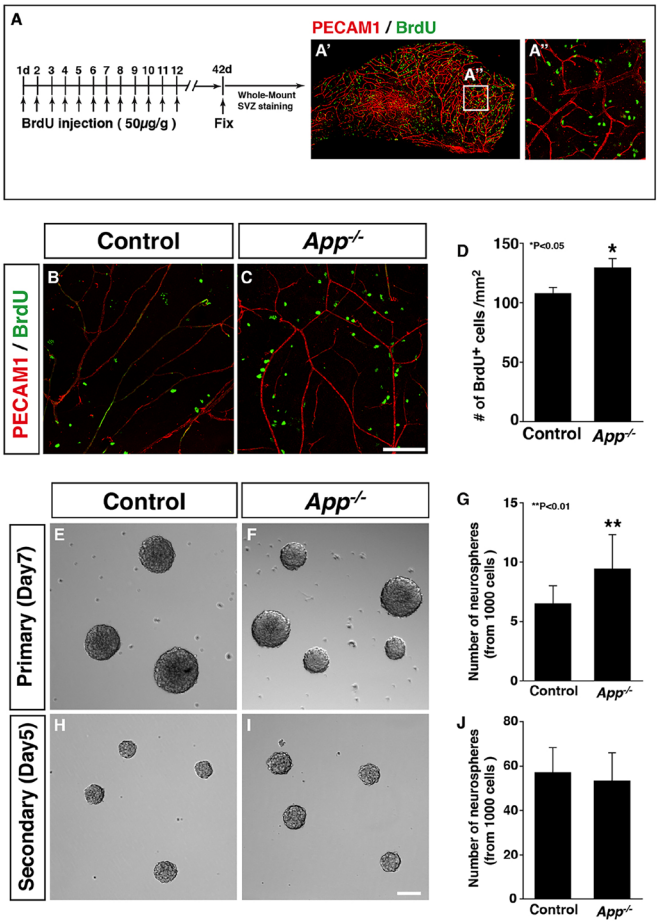

Fig. 3. APP negatively regulates SVZ-NSC number in a non-cell-autonomous manner. (A-A″) Experimental design for a label-retention assay using BrdU in the adult SVZ (A) and whole-mount staining of SVZ with antibodies to the pan-endothelial marker PECAM1 (red) and BrdU indicating label-retaining NSCs (green) (A′,A″). (B,C) Whole-mount staining of *App* mutants and their control littermates with antibodies to PECAM1 (red) and BrdU (green). (D) Quantification of BrdU$^+$ label-retaining NSCs per mm^2. *P<0.05 (Student's t-test). n=18, control SVZ tissues; n=14, mutant SVZ tissues from 7-9 animals. Bars represent mean±s.e.m. (E,F) Images of typical primary neurospheres from acutely dissociated control or *App* mutant SVZ. (G) Quantification of primary neurosphere number. n=14, control; n=15, *App* null mutants from three independent experiments. Bars represent mean±s.d. **P<0.01 (Student's t-test). (H,I) Images of typical secondary neurospheres derived from control or *App* null SVZ-derived primary neurospheres. (J) Quantification of the secondary neurosphere number. n=15, control; n=15, *App* null mutants from three independent experiments. Bars represent mean±s.d. Scale bars:100 µm.

Development (2017) 144, 2730-2736 doi:10.1242/dev.143370

significant increase in the number of BrdU$^+$ label-retaining NSCs in the SVZ, compared with control littermates (Fig. 3B-D). In support of this observation, the mutants yielded more primary neurospheres than did control littermates (Fig. 3E-G). However, there was no significant difference in the number of secondary neurospheres on subcloning (Fig. 3H-J), suggesting that APP negatively regulates NSC number in a non-cell-autonomous manner.

Endothelial APP functions as a negative regulator to control SVZ-NSC number *in vivo*

To address directly whether EC-derived APP controls NSC number *in vivo*, we bred *App*$^{flox/flox}$ mice (Callahan et al., 2017) with an EC-specific *Cre* driver, *Tie2-Cre* (Kisanuki et al., 2001), and an NSC/astrocyte-specific *Cre* driver, *GFAP-Cre* (Zhuo et al., 2001), producing *App*$^{flox/flox}$*;Tie2-Cre* mice and *App*$^{flox/flox}$*;GFAP-Cre* mice, respectively. As seen in the conventional *App* null mutants, more BrdU$^+$ label-retaining NSCs were detected in the SVZ of *App*$^{flox/flox}$*;Tie2-Cre* mice (Fig. 4A-C). In contrast, no change in NSC number was seen in the SVZ of *App*$^{flox/flox}$*;GFAP-Cre* mice (Fig. 4D-F). These data clearly indicate an important role for endothelial APP in determining NSC number in the SVZ.

APP deficiency does not detectably influence SVZ architecture and neuronal differentiation

No significant change in the pinwheel-like arrangement of GFAP$^+$ NSCs, β-catenin$^+$ ependymal cells (Fig. S6A,B) or the SVZ microvascular network (Fig. S6C-E) was observed in *App* mutants. Moreover, the mutants showed no significant change in the amount of doublecortin (DCX)$^+$ neuroblasts (Fig. S6F-H) and Mash1 (Ascl1)$^+$/Ki67 (Mki67)$^+$ transit-amplifying cells in the SVZ (Fig. S6I-K). Likewise, no significant change in the amount of NeuN (Rbfox3)$^+$ post-mitotic neurons in the olfactory bulb was observed (Fig. S6L-O). One possible explanation is that the ∼20% increase in the number of SVZ-NSCs might be overridden by the subsequent expansion of SVZ neural progenitors and the migration of SVZ neuroblasts to the olfactory bulb. These relatively subtle but significant phenotypes in conventional and *App* mutants could indicate that other APP family members may compensate for the loss of APP. Previous studies in mice suggest functional redundancy between APP and APP-like protein 2 (APLP2): APLP2 can take over APP functions *in vivo* (van der Kant and Goldstein, 2015). Indeed, APLP2 was found in the 29 proteins from the bEND3 derived-CM fraction (Fig. S2B) and was also identified from our secreted molecule profiling of the adult SVZ ECs (Lee et al., 2012). It would be interesting to study the functional redundancy between APP and APLP2 by analysis of *App*$^{-/-}$*;Aplp2*$^{-/-}$ double knockout mice.

Conclusions

We present here a normal cell biological role of APP as a negative regulator of NSC growth to control NSC number in the adult SVZ. Given that the major source of SVZ-neurosphere-forming cells are actively dividing *in vivo* and include EGF-responsive activated NSCs but not BrdU$^+$ label-retaining quiescent NSCs (Codega et al., 2014), the observations that sAPP treatment increases the number of neurospheres in culture (our studies) and neurosphere-forming cells *in vivo* (Caille et al., 2004) can be explained by the positive effect of sAPP on the neurosphere-forming potential of activated NSCs. By contrast, sAPP negatively regulates the growth of quiescent NSCs *in vivo* (our studies). These results raise one intriguing question: if sAPP treatment enhances the neurosphere-forming potential in activated NSCs, why does *App* deficiency lead to an increase in the number of neurosphere-forming cells in the SVZ? One possible explanation is that sAPP may be sufficient, but not necessary, to enhance the neurosphere-forming potential *in vivo*: in the *App* mutants, an increase in the number of quiescent NSCs may lead to an increase in the number of neurosphere-forming activated NSCs.

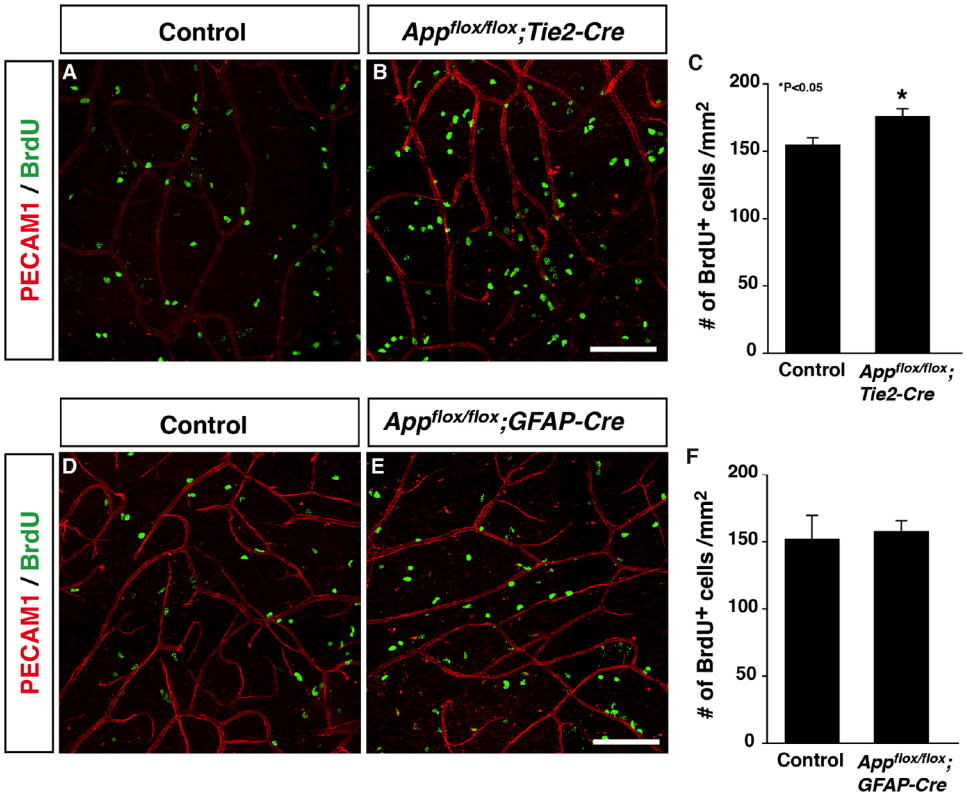

Fig. 4. Endothelial APP is responsible for SVZ-NSC number. (A-C) Whole-mount staining of *App*$^{flox/flox}$*;Tie2-Cre* mutants and their control littermates with antibodies to PECAM1 (red) and BrdU (green) (A,B) and quantification of BrdU$^+$ label-retaining NSCs per mm^2 (C). *P<0.05 (Student's t-test). n=12, control SVZ tissues; n=10, *App*$^{flox/flox}$*;Tie2-Cre* mutant SVZ tissues from 5-6 animals. Bars represent mean±s.e.m. (D-F) Whole-mount staining of *App*$^{flox/flox}$*;GFAP-Cre* mutants and their control littermates with antibodies to PECAM1 (red) and BrdU (green) (D,E) and quantification of BrdU$^+$ label-retaining NSCs per mm^2 (F). n=12, control; n=12, *App*$^{flox/flox}$*;GFAP-Cre* mutants from 6 animals. Bars represent mean±s.e.m. Scale bars:100 µm.

Development (2017) 144, 2730-2736 doi:10.1242/dev.143370

Identification of NSC receptors for sAPP will provide a clearer understanding of the mechanisms by which sAPP regulates the cellular processes of quiescent and activated NSC behaviors.

MATERIALS AND METHODS

Animals

C57BL/6 mice (The Jackson Laboratory), *App* mutants (Zheng et al., 1995) (The Jackson Laboratory), $App^{flox/flox}$ mutants (Callahan et al., 2017), *Tie2-Cre* mice (Kisanuki et al., 2001), *GFAP-Cre* mice (Zhuo et al., 2001) (The Jackson Laboratory), and *Flk1-GFP BAC Tg* mice (Ishitobi et al., 2010) have been reported elsewhere. All experiments were carried out according to the guidelines approved by the National Heart, Lung, and Blood Institute Animal Care and Use Committee.

Preparation of CM from bEND3 cells

bEND3 cells (ATCC) were cultured in the ATCC formulated Dulbecco's Modified Eagle's Medium (DMEM, Gibco/Thermo Fisher Scientific) containing 10% fetal bovine serum (Hyclone Laboratories) and Penicillin-Streptomycin (Gibco/Thermo Fisher Scientific). Preparation of bEND3-derived CM is provided in supplementary Materials and Methods.

Recombinant proteins

The secreted forms of control alkaline phosphatase (AP) and APP were prepared for the neurosphere assay. For details, see supplementary Materials and Methods.

Heparin-agarose fractionation

A total of 500 ml of bEND3 CM was applied to Heparin-Agarose (5 ml bed volume, Sigma). After washing of the column by PBS, the bound proteins were eluted by 30 ml of different concentration of NaCl solution (from 200 mM to 500 mM, every 50 mM). The eluted proteins were concentrated with buffer exchange to PBS through the centrifugal filter unit (Amicon ultra 10K MWCO, Millipore). Each fraction was tested in the neurosphere assay.

Neurosphere culture

Neurospheres were established and cultured as described previously (Ferron et al., 2007) with slight modifications. For details, see supplementary Materials and Methods.

Cell viability assay

Viability of NSCs was assessed as described previously (Ferron et al., 2007). For details, see supplementary Materials and Methods and Table S1.

BrdU labeling and immunohistochemistry

BrdU labeling and whole-mount SVZ immunohistochemistry were performed essentially as described previously (Shen et al., 2008; Tavazoie et al., 2008). All confocal microscopy analysis was carried out on a Leica TCS SP5 confocal (Leica). For details and antibody information, see supplementary Materials and Methods and Table S1.

Flow cytometry

To isolate SVZ and cortex endothelial cells, we used *Flk1-GFP* endothelial cell reporter mice (Ishitobi et al., 2010). All sorting was performed with a FACS Aria (Becton Dickinson). For details, see supplementary Materials and Methods.

RT-PCR

Total RNA was isolated using TRIzol reagent (Ambion) or the RNeasy Mini Kit (QIAGEN) according to the manufacturer's instructions, and reverse-transcribed using SuperScript III (Invitrogen) for PCR. For details and primer information, see supplementary Materials and Methods.

Statistical analysis

Quantification data are represented as means±s.d., means±s.e.m. or box-and-whisker plots. *P*-values were calculated by Student's *t*-test, with $P<0.05$ considered significant. For comparisons across more than two groups, data were analyzed using one-way analysis of variance (ANOVA) with Tukey-HSD multiple comparison test or two-way ANOVA with Sidak correction for multiple comparisons.

Acknowledgements

We thank Y. Chen and M. Gucek for LC-MS assistance; J. Hawkins and the staff of NIH Bldg50 and Bldg14F animal facility for assistance with mouse breeding and care; P. J. McCoy and the staff of the Flow Cytometry Core for FACS assistance; K. Gill for laboratory management and technical support; and R. Reed and F. Baldrey for administrative assistance. Thanks also to R. Adelstein for editorial help and discussion; W. Li for technical help; and S. Kim, B.-N. Koo, J. Msefya, L. Henderson and other members of the Laboratory of Stem Cell and Neuro-Vascular Biology for valuable help and discussion.

Competing interests

The authors declare no competing or financial interests.

Author contributions

Conceptualization: Y.M.; Methodology: Y.S., Y.U., J.H.; Validation: Y.S., Y.U.; Formal analysis: Y.S., Y.U.; Investigation: Y.S., Y.U.; Resources: T.L.Y.-P., T.N.; Writing - original draft: Y.U., Y.M.; Writing - review & editing: Y.S., Y.U., Y.M.; Supervision: Y.M.; Project administration: Y.M.; Funding acquisition: Y.M.

Funding

This work was supported by the Intramural Research Program of the National Heart, Lung, and Blood Institute, National Institutes of Health (HL006115-06 to Y.M.). Deposited in PMC for release after 12 months.

Supplementary information

Supplementary information available online at
http://dev.biologists.org/lookup/doi/10.1242/dev.143370.supplemental

References

Baratchi, S., Evans, J., Tate, W. P., Abraham, W. C. and Connor, B. (2012). Secreted amyloid precursor proteins promote proliferation and glial differentiation of adult hippocampal neural progenitor cells. *Hippocampus* **22**, 1517-1527.

Caille, I., Allinquant, B., Dupont, E., Bouillot, C., Langer, A., Muller, U. and Prochiantz, A. (2004). Soluble form of amyloid precursor protein regulates proliferation of progenitors in the adult subventricular zone. *Development* **131**, 2173-2181.

Callahan, D. G., Taylor, W. M., Tilearcio, M., Cavanaugh, T., Selkoe, D. J. and Young-Pearse, T. L. (2017). Embryonic mosaic deletion of APP results in displaced Reelin-expressing cells in the cerebral cortex. *Dev. Biol.* **424**, 138-146.

Codega, P., Silva-Vargas, V., Paul, A., Maldonado-Soto, A. R., Deleo, A. M., Pastrana, E. and Doetsch, F. (2014). Prospective identification and purification of quiescent adult neural stem cells from their in vivo niche. *Neuron* **82**, 545-559.

Crouch, E. E., Liu, C., Silva-Vargas, V. and Doetsch, F. (2015). Regional and stage-specific effects of prospectively purified vascular cells on the adult V-SVZ neural stem cell lineage. *J. Neurosci.* **35**, 4528-4539.

Delgado, A. C., Ferron, S. R., Vicente, D., Porlan, E., Perez-Villalba, A., Trujillo, C. M., D'Ocon, P. and Farinas, I. (2014). Endothelial NT-3 delivered by vasculature and CSF promotes quiescence of subependymal neural stem cells through nitric oxide induction. *Neuron* **83**, 572-585.

Ferron, S. R., Andreu-Agullo, C., Mira, H., Sanchez, P., Marques-Torrejon, M. A. and Farinas, I. (2007). A combined ex/in vivo assay to detect effects of exogenously added factors in neural stem cells. *Nat. Protoc.* **2**, 849-859.

Gomez-Gaviro, M. V., Scott, C. E., Sesay, A. K., Matheu, A., Booth, S., Galichet, C. and Lovell-Badge, R. (2012). Betacellulin promotes cell proliferation in the neural stem cell niche and stimulates neurogenesis. *Proc. Natl. Acad. Sci. USA* **109**, 1317-1322.

Guo, Q., Li, H., Gaddam, S. S. K., Justice, N. J., Robertson, C. S. and Zheng, H. (2012). Amyloid precursor protein revisited: neuron-specific expression and highly stable nature of soluble derivatives. *J. Biol. Chem.* **287**, 2437-2445.

Ishitobi, H., Matsumoto, K., Azami, T., Itoh, F., Itoh, S., Takahashi, S. and Ema, M. (2010). Flk1-GFP BAC Tg mice: an animal model for the study of blood vessel development. *Exp. Anim.* **59**, 615-622.

Jung, S., Park, R.-H., Kim, S., Jeon, Y.-J., Ham, D.-S., Jung, M.-Y., Kim, S.-S., Lee, Y.-D., Park, C.-H. and Suh-Kim, H. (2010). Id proteins facilitate self-renewal and proliferation of neural stem cells. *Stem Cells Dev.* **19**, 831-841.

Kisanuki, Y. Y., Hammer, R. E., Miyazaki, J.-I., Williams, S. C., Richardson, J. A. and Yanagisawa, M. (2001). Tie2-Cre transgenic mice: a new model for endothelial cell-lineage analysis in vivo. *Dev. Biol.* **230**, 230-242.

Kriegstein, A. and Alvarez-Buylla, A. (2009). The glial nature of embryonic and adult neural stem cells. *Annu. Rev. Neurosci.* **32**, 149-184.

Lee, C., Hu, J., Ralls, S., Kitamura, T., Loh, Y. P., Yang, Y., Mukouyama, Y.-S. and Ahn, S. (2012). The molecular profiles of neural stem cell niche in the adult subventricular zone. *PLoS ONE* **7**, e50501.

Leventhal, C., Rafii, S., Rafii, D., Shahar, A. and Goldman, S. A. (1999). Endothelial trophic support of neuronal production and recruitment from the adult mammalian subependyma. *Mol. Cell. Neurosci.* **13**, 450-464.

Ma, Q.-H., Futagawa, T., Yang, W.-L., Jiang, X.-D., Zeng, L., Takeda, Y., Xu, R.-X., Bagnard, D., Schachner, M., Furley, A. J. et al. (2008). A TAG1-APP signalling pathway through Fe65 negatively modulates neurogenesis. *Nat. Cell Biol.* **10**, 283-294.

Ming, G.-L. and Song, H. (2005). Adult neurogenesis in the mammalian central nervous system. *Annu. Rev. Neurosci.* **28**, 223-250.

Nam, H.-S. and Benezra, R. (2009). High levels of Id1 expression define B1 type adult neural stem cells. *Cell Stem Cell* **5**, 515-526.

Ohsawa, I., Takamura, C., Morimoto, T., Ishiguro, M. and Kohsaka, S. (1999). Amino-terminal region of secreted form of amyloid precursor protein stimulates proliferation of neural stem cells. *Eur. J. Neurosci.* **11**, 1907-1913.

Olsen, O., Kallop, D. Y., McLaughlin, T., Huntwork-Rodriguez, S., Wu, Z., Duggan, C. D., Simon, D. J., Lu, Y., Easley-Neal, C., Takeda, K. et al. (2014). Genetic analysis reveals that amyloid precursor protein and death receptor 6 function in the same pathway to control axonal pruning independent of beta-secretase. *J. Neurosci.* **34**, 6438-6447.

Ottone, C., Krusche, B., Whitby, A., Clements, M., Quadrato, G., Pitulescu, M. E., Adams, R. H. and Parrinello, S. (2014). Direct cell-cell contact with the vascular niche maintains quiescent neural stem cells. *Nat. Cell Biol.* **16**, 1045-1056.

Palmer, T. D., Willhoite, A. R. and Gage, F. H. (2000). Vascular niche for adult hippocampal neurogenesis. *J. Comp. Neurol.* **425**, 479-494.

Rafii, S., Butler, J. M. and Ding, B.-S. (2016). Angiocrine functions of organ-specific endothelial cells. *Nature* **529**, 316-325.

Ramirez-Castillejo, C., Sanchez-Sanchez, F., Andreu-Agullo, C., Ferron, S. R., Aroca-Aguilar, J. D., Sanchez, P., Mira, H., Escribano, J. and Farinas, I. (2006). Pigment epithelium-derived factor is a niche signal for neural stem cell renewal. *Nat. Neurosci.* **9**, 331-339.

Shen, Q., Goderie, S. K., Jin, L., Karanth, N., Sun, Y., Abramova, N., Vincent, P., Pumiglia, K. and Temple, S. (2004). Endothelial cells stimulate self-renewal and expand neurogenesis of neural stem cells. *Science* **304**, 1338-1340.

Shen, Q., Wang, Y., Kokovay, E., Lin, G., Chuang, S.-M., Goderie, S. K., Roysam, B. and Temple, S. (2008). Adult SVZ stem cells lie in a vascular niche: a quantitative analysis of niche cell-cell interactions. *Cell Stem Cell* **3**, 289-300.

Tavazoie, M., Van der Veken, L., Silva-Vargas, V., Louissaint, M., Colonna, L., Zaidi, B., Garcia-Verdugo, J. M. and Doetsch, F. (2008). A specialized vascular niche for adult neural stem cells. *Cell Stem Cell* **3**, 279-288.

van der Kant, R. and Goldstein, L. S. (2015). Cellular functions of the amyloid precursor protein from development to dementia. *Dev. Cell* **32**, 502-515.

Wang, B., Wang, Z., Sun, L., Yang, L., Li, H., Cole, A. L., Rodriguez-Rivera, J., Lu, H.-C. and Zheng, H. (2014). The amyloid precursor protein controls adult hippocampal neurogenesis through GABAergic interneurons. *J. Neurosci.* **34**, 13314-13325.

Wang, S., Bolos, M., Clark, R., Cullen, C. L., Southam, K. A., Foa, L., Dickson, T. C. and Young, K. M. (2016). Amyloid beta precursor protein regulates neuron survival and maturation in the adult mouse brain. *Mol. Cell. Neurosci.* **77**, 21-33.

Willem, M., Tahirovic, S., Busche, M. A., Ovsepian, S. V., Chafai, M., Kootar, S., Hornburg, D., Evans, L. D., Moore, S., Daria, A. et al. (2015). eta-Secretase processing of APP inhibits neuronal activity in the hippocampus. *Nature* **526**, 443-447.

Zhao, C., Deng, W. and Gage, F. H. (2008). Mechanisms and functional implications of adult neurogenesis. *Cell* **132**, 645-660.

Zheng, H., Jiang, M., Trumbauer, M. E., Sirinathsinghji, D. J. S., Hopkins, R., Smith, D. W., Heavens, R. P., Dawson, G. R., Boyce, S., Conner, M. W. et al. (1995). beta-Amyloid precursor protein-deficient mice show reactive gliosis and decreased locomotor activity. *Cell* **81**, 525-531.

Zhuo, L., Theis, M., Alvarez-Maya, I., Brenner, M., Willecke, K. and Messing, A. (2001). hGFAP-cre transgenic mice for manipulation of glial and neuronal function in vivo. *Genesis* **31**, 85-94.

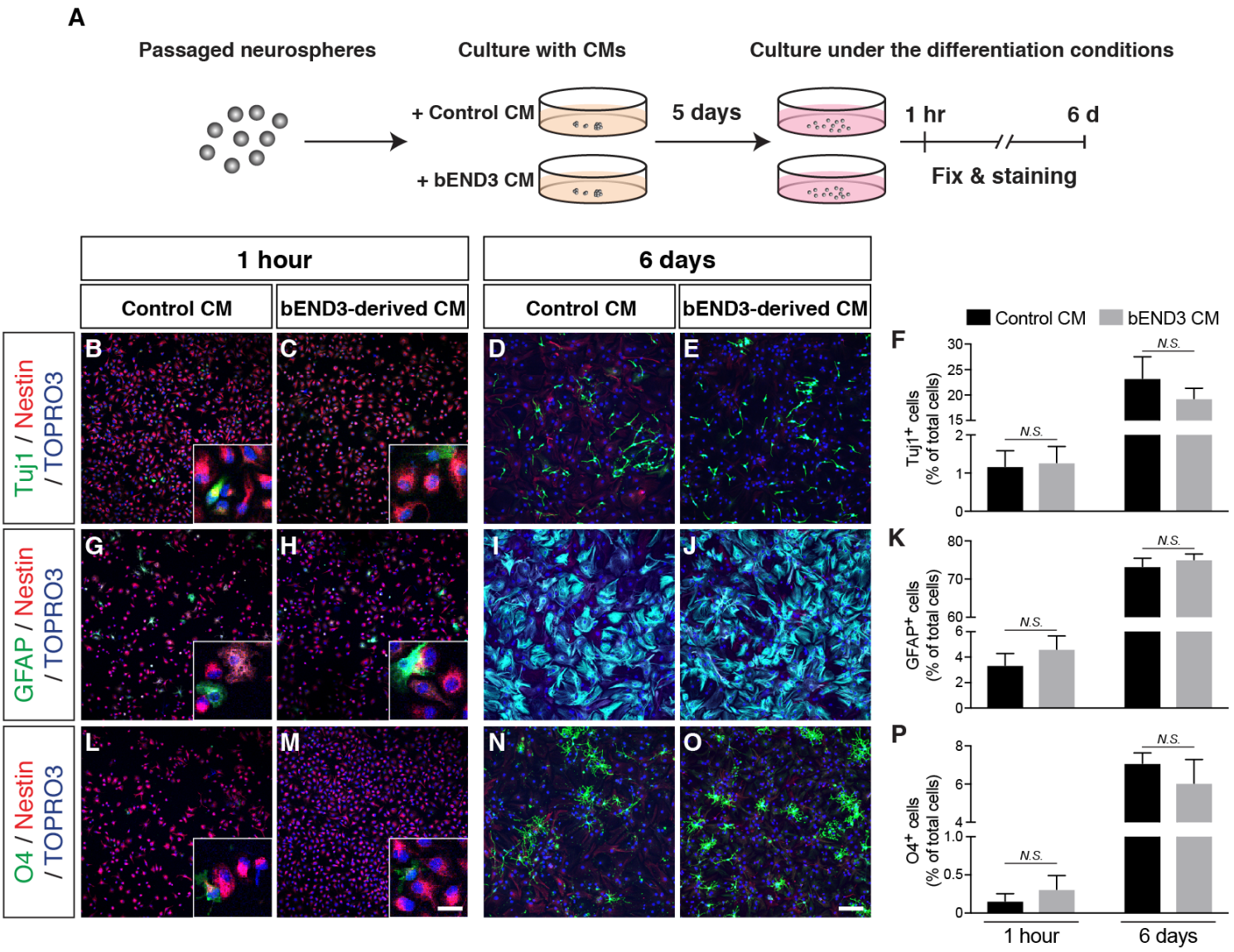

Figure S1. Differentiation capacity of neurospheres following exposure to bEND3-CM

(A) A schematic model of the experimental design.

(B-F) Representative images showing the differentiation of passaged neurospheres into neurons. Neurospheres after exposure to control CM or bEND3-CM were replated in the differentiating conditions and cultured for 1 hour (B, C) or 6 days (D, E), followed by

immunostaining with Tuj1 (green) together with anti-nestin (red) as a marker for undifferentiated cells. Nuclei were stained with TOPRO3 (blue). Quantification of $Tuj1^+$ neurons is shown in (F). Data represents the mean ± SEM of 6 randomly obtained images from two independent experiments.

(G-K) Representative images showing the differentiation of passaged neurospheres into astrocytes. Neurospheres after exposure to control CM or bEND3-CM were replated in the differentiating condition and cultured for 1 hour (G, H) or 6 days (I, J), followed by immunostaining with anti-GFAP (green) together with anti-nestin (red) as a marker for undifferentiated cells. Nuclei were stained with TOPRO3 (blue). Quantification of $GFAP^+$ astrocytes is shown in (K). Data represents the mean ± SEM of 6 randomly obtained images from two independent experiments.

(L-P) Representative images showing the differentiation of passaged neurospheres into oligodendrocytes. Neurospheres after exposure to control CM or bEND3-CM were replated in the differentiating condition and cultured for 1 hour (L, M) or 6 days (N, O), followed by immunostaining with anti-O4 (green) together with anti-nestin (red) as a marker for undifferentiated cells. Nuclei were stained with TOPRO3 (blue). Quantification of $O4^+$ oligodendrocytes is shown in (P). Scale bar, 20 μm (M, inset) and 100 μm (O). Data represents the mean ± SEM of 6 randomly obtained images from two independent experiments. *N.S.*, not significant according to two-way ANOVA with Sidak multiple comparisons test.

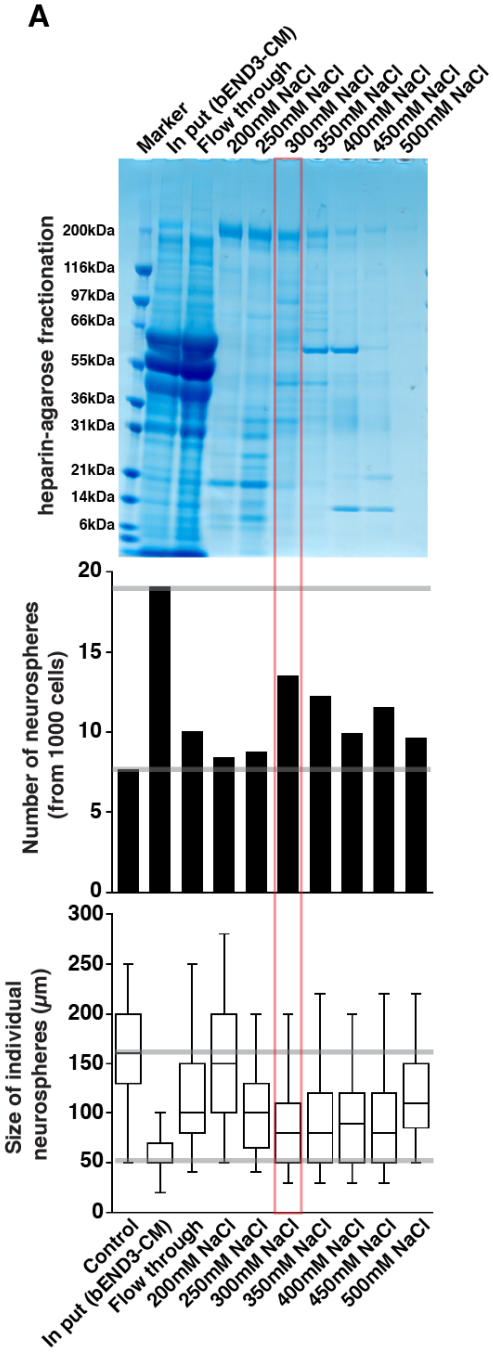

B

	Name	Accession Number	Effects	
			Number	Size
	A disintegrin and metalloproteinase with thrombospondin motifs 1 (ADAM-TS1)	ATS1_MOUSE	N.E (no effect)	N.E
*	Amyloid beta A4 protein	A4_MOUSE	N.E	Decrease
*	Amyloid-like protein 2	APLP2_MOUSE	N.E	Decrease
	Antithrombin-III	ANT3_MOUSE	- (not tested)	-
	Basement membrane-specific heparan sulfate proteoglycan core protein	PGBM_MOUSE	-	-
	Calsyntenin-1	CSTN1_MOUSE	N.E	Decrease
	Collagen alpha-1(V) chain	CO5A1_MOUSE	-	-
	Collagen alpha-1(XVIII) chain	COIA1_MOUSE	-	-
	Collagen alpha-2(IV) chain	CO4A2_MOUSE	-	-
	Extracellular matrix protein 1	ECM1_MOUSE	-	-
	Fibronectin	FINC_MOUSE	N.E	N.E
	Inhibin beta B chain	INHBB_MOUSE	Increase	Decrease
	Insulin-like growth factor-binding protein 3	IBP3_MOUSE	N.E	N.E
	Insulin-like growth factor-binding protein 9 (Protein NOV homolog)	NOV_MOUSE	-	-
	Integrin beta-1	ITB1_MOUSE	-	-
	Lactadherin (MFG-E8)	MFGM_MOUSE	N.E	N.E
*	Laminin subunit alpha-4	LAMA4_MOUSE	-	-
	Lysyl oxidase homolog 4	LOXL4_MOUSE	-	-
	Nephronectin	NPNT_MOUSE	Increase	Increase
	Neuropilin-1	NRP1_MOUSE	-	-
	Nidogen-1	NID1_MOUSE	-	-
	Peroxidasin homolog	PXDN_MOUSE	N.E	N.E
	Receptor-type tyrosine-protein phosphatase beta (VE-PTP)	PTPRB_MOUSE	-	-
	Receptor-type tyrosine-protein phosphatase S	PTPRS_MOUSE	-	-
	Reticulon-4 (NogoA)	RTN4_MOUSE	N.E	Decrease
	Stanniocalcin-1	STC1_MOUSE	-	-
	Transcobalamin-2	TCO2_MOUSE	N.E	N.E
	Transmembrane protein 132A	T132A_MOUSE	-	-
	Urokinase-type plasminogen activator	UROK_MOUSE	-	-

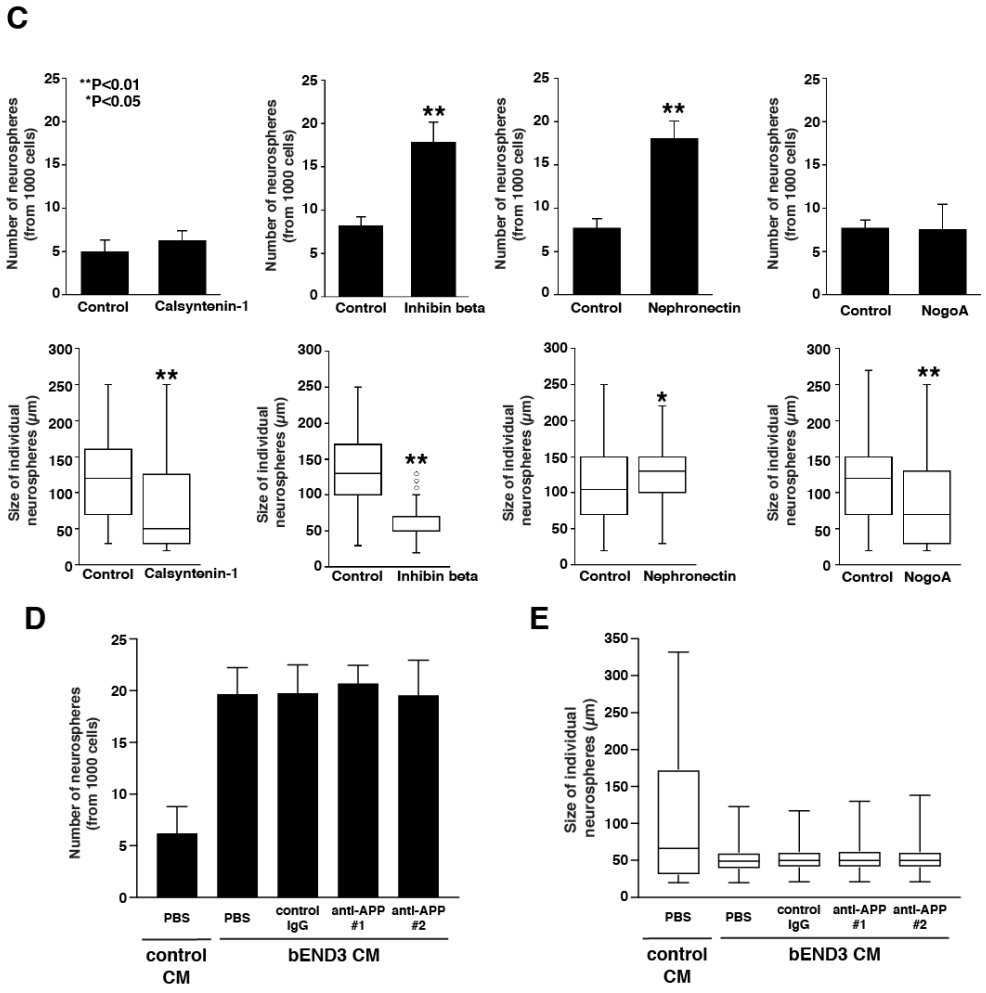

Figure S2. Identification of soluble proteins from bEND3 CM by heparin-agarose fractionation

(A) Fractionation of bEND3-CM by heparin-agarose chromatography and subsequent neurosphere assay: neurospheres from acutely dissociated SVZs were used. Each fraction was tested in the neurosphere assay with the number of neurospheres and the size of individual neurospheres. Note that the most striking reduction in the size of individual neurospheres was observed in the 300 mM-fraction.

(B) List of soluble proteins in the 300 mM-fraction by the LC-MS analysis. Some soluble proteins were further tested in the neurosphere assay. Asterisk indicates that these proteins were also identified from our secreted molecule profiling of SVZ ECs (Lee at al. *PLoS One*, 2012).

(C) Neurosphere assay with representative soluble proteins (1 μg/ml Calsyntenin-1, 0.2 μg/ml inhibin β, 0.5 μg/ml Nephronectin, 1 μg/ml NogoA) were shown. Asterisk indicates statistical significance (*P<0.05; **P<0.01) according to student-t test.

(D-E) Quantification of the number of neurospheres (D) and the size of individual neurospheres (E). Acutely dissociated SVZ cells were plated on a low attachment 96-well plate with control or bEND3-CM in the presence of antibodies against APP (anti-APP #1 is an antibody from ThermoFisher Scientific Inc.; anti-APP #2 is an antibody from Abcam) for 7 days.

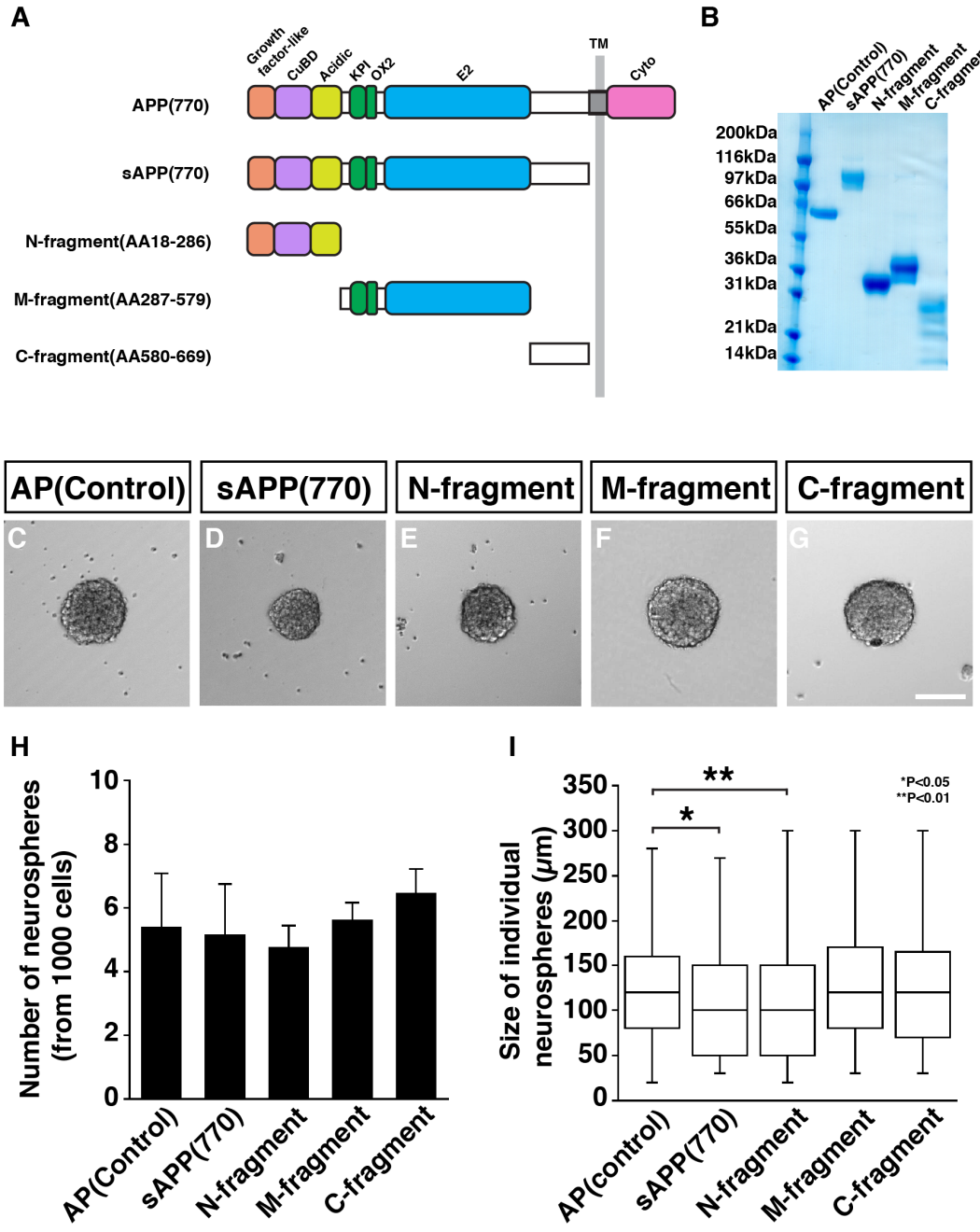

Figure S3. Soluble APP as a vascular niche factor in culture

(A) A schematic diagram depicting major domains in the APP(770) isoform and sAPP fragments.

(B) CBB staining of sAPP fragments. Alkaline phosphatase (AP) as control.

(C-G) Images of typical neurospheres in the medium containing different forms of sAPP fragments. Note that neurospheres from acutely dissociated SVZs were used.

(H) Quantification of the neurosphere number (N=8 from three independent experiments, Bars represent mean ± s.d.).

(I) Quantification of the neurosphere size. Data represented as box and whisker plot. Asterisk indicates statistical significance (*P<0.05; **P<0.01) according to One-Way Analysis of Variance (ANOVA) with Tukey-HSD multiple comparison test. (N=160, AP control; N=197, sAPP; N=199, N-fragment; N=175, M-fragment; N=211, C-fragment from three independent experiments). Scale bar = 100 μm.

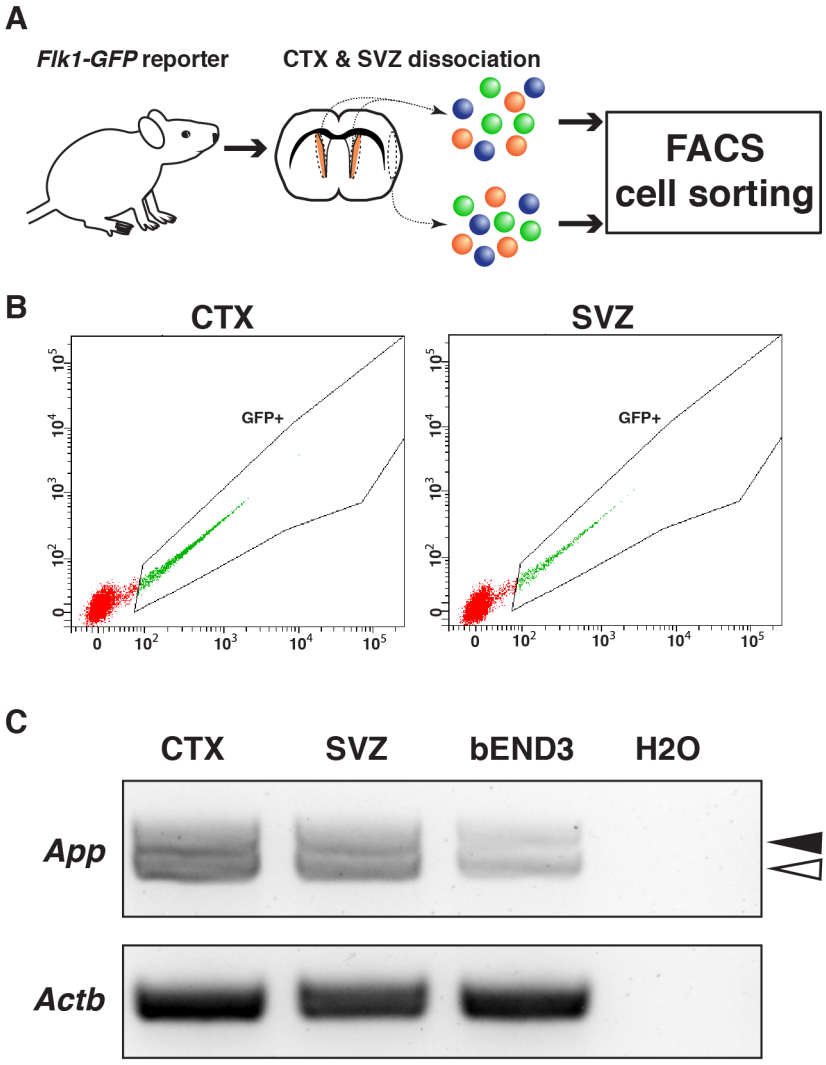

Figure S4. APP expression in SVZ endothelial cells

(A) A schematic model of the experimental design. SVZs and cortex (CTX) ECs were isolated from the adult brain of *Flk1-GFP* EC reporter mice.

(B) FACS isolation of Flk1-GFP^{+} ECs from CTX (left) and SVZ (right).

(C) RT-PCR analysis of *App* and *Actb* (ß-actin) expression in FACS-isolated CTX and SVZ ECs, and cultured bEND3 ECs. Total RNAs extracted from bEND3 ECs were used as a positive control. These ECs express *App* splice variants: closed arrowhead (a 421 bp) corresponding to the *App* variant 1, 2, and 3 mRNAs; open arrowhead (a 367 bp) corresponding to the *App* variant 5, 6, and X1 mRNAs.

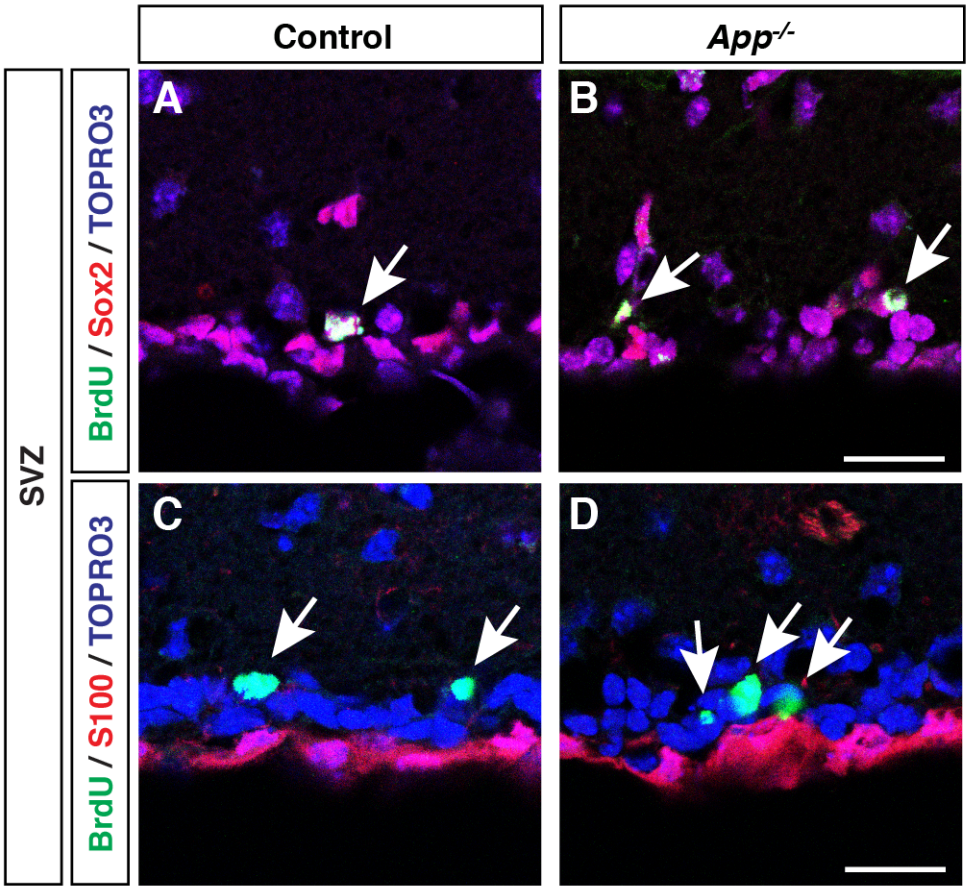

Figure S5. The analysis of BrdU-positive NSCs and their progenies in *App* mutants

A marker profile of BrdU$^+$ label-retaining NSCs in the SVZ of *App* mutants and their control littermates. Immunostaining with antibodies to BrdU (A-D, green), a NSC marker Sox2 (A, B, red) and an ependymal cell marker S100 (C, D, red), together with a nuclear marker TOPRO3 (A-D, blue). Note that the BrdU$^+$ label-retaining NSCs (arrowheads) are positive for Sox2 but negative for S100 in *App* mutants and their control littermates. Scale bar = 50 μm.

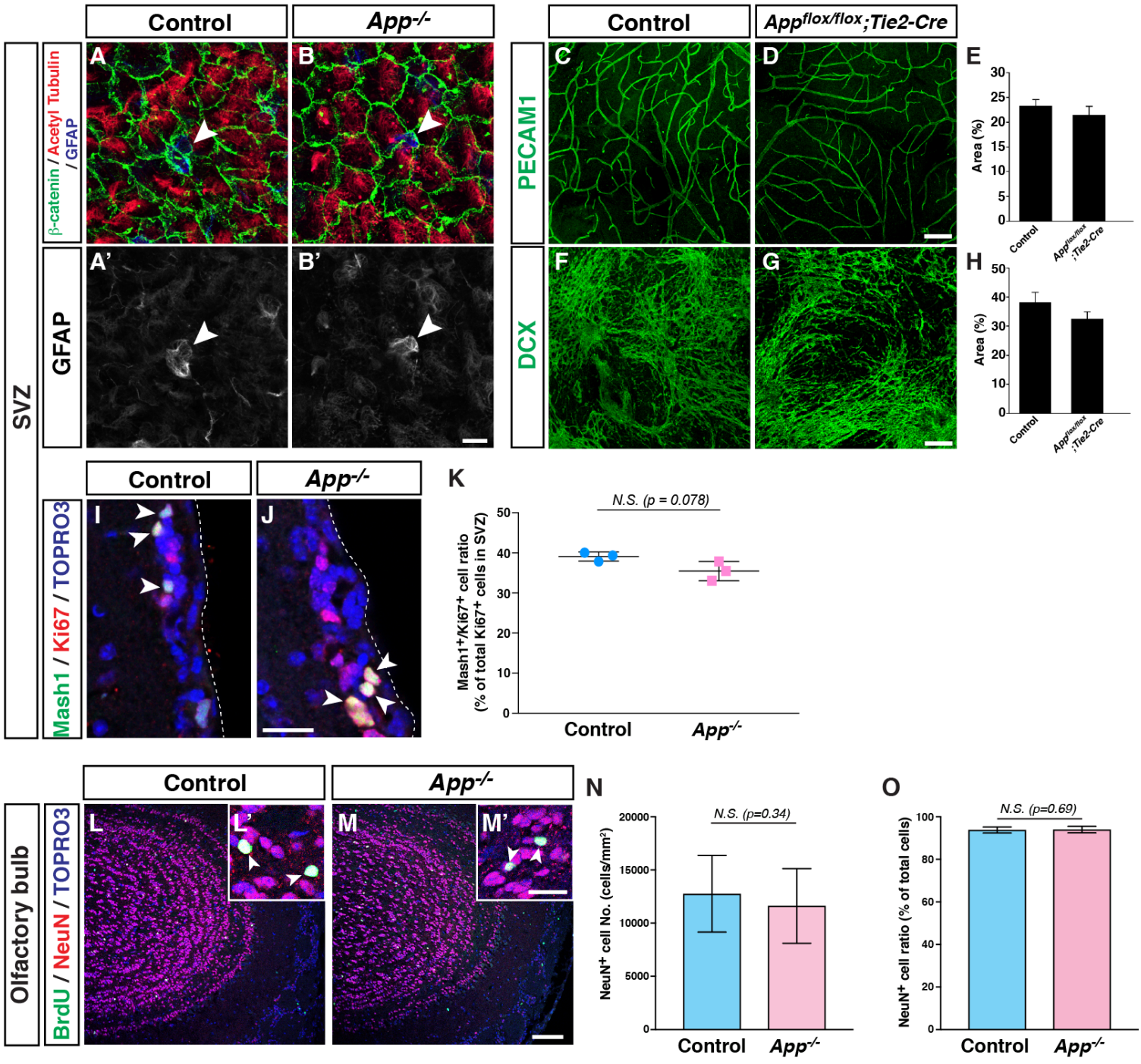

Figure S6. The morphological analysis of SVZs in *App* mutants

(A, B) Whole mount SVZs staining of *App* mutants (B, B') and their control littermates (A, A') with antibodies to an ependymal/NSC cell-cell junction marker β-catenin (A, B, green), an ependymal cilia marker acetylated tubulin (A, B, red), and a NSC/astrocyte marker GFAP (A, B, blue; A', B', white). A center of pinwheel structure is characteristic of NSC localization (arrowhead, Mirzadeh et al., 2008). Scale bar = 10 μm.

(C-E) Whole mount SVZs staining of *App* mutants (D) and their control littermates (C) with antibody to pan-endothelial cell marker PECAM-1. Scale bar = 100 μm. Quantification of PECAM1 positive area in the SVZ (E).

(F-H) Whole mount SVZs staining of *App* mutants (G) and their control littermates (F) with antibody to a neuroblast marker doublecortin (Dcx). Scale bar = 100 μm. Quantification of Dcx-positive area in the SVZ (H).

(I-K) Immunostaining of SVZs from *App* mutants (I) and their control littermates (J) with antibodies to a transit amplifying cell marker Mash1 (green) and a mitotic cell marker Ki67 (red), together with TOPRO3 (blue). Arrowheads indicate $Mash1^{+}Ki67^{+}$ type-C transit amplifying cells. Dotted lines indicate the lateral ventricular wall. Scale bar = 20 μm. (K) Quantification of the type-C transit amplifying cells. Mash1/Ki67 double positive cells per total Ki67 positive mitotic cells in the SVZs is shown. Data represents the mean ± s.d. of three independent experiments from three control and $App^{-/-}$ mice, respectively.

(L-O) Immunostaininig of the olfactory bulb from *App* mutants (M, M') and their control littermates (L, L') with antibodies to BrdU (L, M, green) and a post-mitotic neuron marker NeuN (L, M, red), together with TOPRO3 (blue). Scale bar = 100 μm. The insets

indicate magnified images (L', M'). The label retention assay using BrdU showed $BrdU^{+}NeuN^{+}$ post-mitotic neurons in the olfactory bulb of *App* mutants (M') and their control littermates (L'). Scale bar = 20 μm. Quantification of the number of $NeuN^{+}$ cells (N) and ratio (O) in the granule cell layer of *App* mutant and their control littermate olfactory bulb. Data represents the mean ± s.d. of three independent experiments (N=26900 from 19 images and N=25225 from 17 images in three control and $App^{-/-}$ mice, respectively).

SUPPLEMENTARY MATERIALS AND METHODS

Preparation of CM from bEND3 cells

bEND3 cells (ATCC) were cultured in 15 cm dish with the ATCC formulated Dulbecco's Modified Eagle's Medium (DMEM, Gibco/Thermo Fisher Scientific) containing 10% FBS (Hyclone Laboratories) and Penicillin-Streptomycin (Gibco/Thermo Fisher Scientific). When the cells reached confluence, the medium was replaced by serum free Opti-MEM (Gibco/Thermo Fisher Scientific) and the cells were cultured for additional 2 days. A total of 100 ml of the medium conditioned by bEND3 cells was collected and concentrated 100-fold with buffer exchange to Phosphate-Buffered Saline (PBS, Gibco/Thermo Fisher Scientific) by using a centrifugal filter unit (Amicon ultra 10K MWCO, Millipore): Note that 100ml of fresh serum free Opti-MEM were concentrated as control CM.

Recombinant proteins

The secreted form of APP (770), N-terminal fragment (AA18-286), M-fragment (AA287-579), and C-terminal fragment (A580-669) were amplified by PCR and subcloned into a modified pAPtag-5 vector (GenHunter) encoding His- and Flag-tag which adds the tags at the N-terminus of APP fragments. The pAPtag-5 expression vector carrying N-terminal His- and FLAG-tagged full length APP(770), fragments of APP, and the vector alone for control AP were transfected into HEK 293T cells (15 cm dish X 20 dishes): APP(770) was cleaved by α-secretase to generate soluble APP(770) in the cells. One day after transfection, the medium was replaced by serum-free Opti-MEM. His-tagged

proteins were purified by TALON metal affinity chromatography (Clontech). Subsequently, the purified proteins went through gel filtration chromatography (Sephacryl S300, Sigma). Fraction materials were concentrated with buffer exchange to PBS through the centrifugal filter unit (Amicon ultra 10K MWCO, Millipore).

Neurosphere culture

The SVZ were dissected from 8-10 week old female brains and dissociated by Papain Dissociation System (Worthington). The cell suspension was triturated and filtered through a 70 μm cell strainer and myelin components were removed by Myelin Removal Beads (Miltenyi Biotec). The SVZ cells were plated on 35-mm petri dish and grown in DMEM/F12 (Gibco/Thermo Fisher Scientific) containing N2 and B27 supplements (Gibco/Thermo Fisher Scientific) in the presence of 20 ng/ml EGF (Peprotech) and bFGF (R&D system) for 5-7 days, and passaged for several times (typically 2-10 times) to concentrate NSCs. For sphere formation assay, neurospheres were dissociated with trypsin-EDTA (ThermoFisher), then 500 cells (at a density of 2 cells/μl) were plated in each well of 96-well ultra low attachment plates (Corning #3474) with x100 control CM, x100 bEND3 CM, rabbit anti-APP antibodies (10 μg/ml; ThermoFisher, PA5-13327; Abcam, ab15272), or purified soluble APP proteins (10 μg/ml) in addition to 5-20 ng/ml EGF and bFGF. The number of neurospheres was counted and the size (diameter) of individual neurospheres was randomly measured from the 5-day culture (at least three independent experiments). Then the neurospheres were dissociated and plated at a density of 2 cells/μl for 5 days to examine secondary sphere formation. For differentiation experiments, neurospheres treated with CM or exogeneous proteins were dissociated and

plated in adherent conditions in an 8-well glass chamber slide (Nunc) coated with poly-L-ornithine (Sigma, 100 μg/ml), fibronectin (BD, 100 μg/ml), and laminin (Sigma, 100 μg/ml) with DMEM/F12 containing N2, B27, and 1% FBS for 1 hour or 6 days. The differentiated cells were fixed and stained with antibodies against nestin (chick polyclonal, Abcam, 1:1000), βIII-tubulin (Tuj1, Covance, 1:500), GFAP (G-A-5, SIGMA, 1:1000), and O4 (Millipore, 1:500).

Cell viability assay

Viability of NSCs was assessed as described previously (Ferron et al., 2007). Neurospheres were collected and dissociated with trypsin-EDTA as described above. The dissociated cells were suspended in PBS and labeled with CellTrace™ far red cell proliferation kit (ThermoFisher) according to the manufacturer's instruction. Then 500-1500 cells (at a density of 2-6 cells/μl) were plated in each well of 96-well ultra low attachment plates (Corning #3474) with CTL/bEnd3 CMs (x100 dilution) or purified proteins (10 μg/ml) in addition to 5-20 ng/ml EGF and bFGF for 24 hours. The cells were harvested, suspended in HEPES-buffered saline (HBS) containing 2.5 mM $CaCl_2$, and incubated with AlexaFluor®488-conjugated Annexin V (ThermoFisher) and 1 μg/ml propidium iodide for 15 min. The cells were washed with HBS containing 2.5 mM $CaCl_2$ and plated on an 8-well chamber slide (Nunc) coated with 100 μg/ml poly-L-ornithine for confocal microscopic observation.

BrdU labeling

BrdU (Sigma) was injected intraperitoneally into 8-10 week old mice (50 μg/g body weight) daily for twelve consecutive days. The mice were sacrificed 30 days after the last injection. The mice were fixed by perfusion fixation with 4% paraformaldehyde (Electron Microscopy Sciences) in PBS (PFA/PBS), and the dissected brains underwent further fixation by 4% PFA/PBS 4°C overnight. All confocal microscopy analysis was carried out on a Leica TCS SP5 confocal (Leica). Note that the Tile Scan function allows us to scan and count $BrdU^+$ label-retaining NSCs in the entire region of the SVZ. We compare the number of $BrdU^+$ label-retaining NSCs per the area of the entire SVZ image (mm^2) between control and mutants.

Immunohistochemistry

Fixed brains were embedded into O.C.T. compound (Sakura Finetek) and snap-frozen in isopentane cooled by liquid nitrogen, and 10-12 μm cryosections were prepared on a cryostat. To detect BrdU-labeled cells, sections were incubated with 2 N HCl for 30 minutes, and then soaked in 0.2 M sodium borate buffer (pH 8.0) for 30 min. The sections were blocked with PBS containing 2% goat serum (Invitrogen) and 0.2% TritonX-100, and then incubated with primary antibodies overnight at 4 ˚C. The sections were then incubated with secondary antibodies, followed by mounting with an anti-fade mounting media (Prolong Gold, Life Technologies). For whole mount neurosphere immunostaining, neurospheres grown in the presence of CM or exogeneous proteins were fixed in PBS containing 4% PFA, blocked with PBS containing 10% donkey serum and 0.2% TritonX-100, then incubated with primary antibodies overnight. The neurospheres were washed 5 times with PBS containing 2% donkey serum and 0.2% TritonX-100,

incubated with appropriate secondary antibodies for 2 hours, then mounted on slides with an anti-fade mounting media. For whole mount SVZ immunostaining, SVZs were dissected from brains after perfusion fixation and immersed with -20 ˚C cold methanol for 20 minutes. The SVZs were soaked into acetone for 20 minutes at -20 ˚C, washed with PBS containing 0.2% TritonX-100, and then blocked with PBS containing 10% goat serum and 0.2% TritonX-100 overnight at 4 ˚C. The SVZs were incubated with primary antibodies for 72 hours and then appropriate secondary antibodies (Jackson ImmunoResearch, 1:500) for 48 hours at 4 ˚C. To detect BrdU-labeled cells in whole mount, the SVZs were dissected from fixed brains and incubated with 2 N HCl for 30 minutes, and then soaked in 0.2 M sodium borate buffer (pH 8.0) for 30 minutes. The samples were blocked with PBS containing 0.2% TritonX-100 and 10% goat serum in PBS, and incubated with primary antibodies overnight at 4 ˚C. The samples were washed with PBS containing 2% goat serum and 0.2% TritonX-100 at room temperature, and then incubated with appropriate secondary antibodies for 5 hours at 4˚C. The samples were mounted on slides with 100 μm spacer (life technologies/Thermo Fisher Scientific) in an anti-fade mounting media (Thermo Fisher). In some cases, the SVZs were dehydrated by graded methanol and then mounted in 1:2 mixed solution of benzyl alcohol (Sigma) and benzyl benzoate (Sigma). All confocal microscopy analysis was carried out on a Leica TCS SP5 confocal (Leica). Primary antibodies used were as follows; anti-BrdU (mouse monoclonal, clone B44, BD Pharmingen, 1:500; rat monoclonal, clone BU1/75, Accurate Chemical & Scientific, 1:500), anti-PECAM1 (rat monoclonal, clone MEC13.3, BD Pharmingen, 1:300), anti-Sox2 (rabbit polyclonal, Stemgent, 1:500; Abcam, 1:1000; goat polyclonal, SantaCruz, 1:500), anti-phospho

histone H3 (rabbit polyclonal, Upstate, 1:250), anti-cleaved caspase-3 (rabbit monoclonal, Cell Signaling, 1:200), anti-S100 (rabbit polyclonal, Dako, 1:1000), anti-NeuN (mouse monoclonal, clone A60, Chemicon, 1:250), anti-Mash1 (mouse monoclonal, clone 24B72D11.1, BD Pharmingen, 1:100), anti-Ki67 (rabbit polyclonal, Abcam, 1:300), anti-β-catenin (rabbit polyclonal, Sigma, 1:1000), anti-acetylated tubulin (mouse monoclonal, clone 6-11B-1, Sigma, 1:1000), anti-GFAP (mouse monoclonal, clone G-A-5, Sigma, 1:1000), anti-doublecortin (rabbit polyclonal, Cell Signaling, 1:500).

Flow cytometry

To isolate SVZ and cortex endothelial cells, we used *Flk1-GFP* endothelial cell reporter mice (Ishitobi et al., 2010). The SVZ and cortex were dissected from the adult brain, digested with papain dissociation system (Worthington), mechanically dissociated by passing through 21- and 26-gauge needles, and filtered through a 70 μm cell strainer. The cell suspension was then incubated with myelin removal beads (Miltenyi Biotec), followed by magnetic separation to remove myelin. To assess cell viability, 7-amino-actinomycin D (7-AAD) was added before sorting with a FACS Aria (Becton Dickinson).

RT-PCR

Total RNAs were extracted from FACS-isolated brain ECs, neurospheres, or bEND3 cells using TRIzol reagent (Ambion) or RNeasy Mini Kit (QIAGEN) according to the manufacturer's instructions. cDNA was generated using SuperScript III First-Strand Synthesis System (Invitrogen), and used as a template for PCR. Densitometry was

performed with Image J and relative band intensity was normalized by ß-actin (*Actb*). The primers used were as follows;

App (sense): 5'-TGA TCT ACG AGC GCA TGA AC-3'

App (antisense): 5'-CCG AAT TCT GCA TCC ATC TT-3'

Actb (sense): 5'-GGA CAT CCG CAA AGA CCT GTA-3'

Actb (antisense): 5'-GCT CAG GAG GAG CAA TGA TCT-3'

Sox2 (sense): 5'-ATG CAC AAC TCG GAG ATC AG-3'

Sox2 (antisense): 5'-TAT AAT CCG GGT GCT CCT TC-3'

Hes1 (sense): 5'-CGG TCT ACA CCA GCA ACA GT-3'

Hes1 (antisense): 5'-CAC ATG GAG TCC GAA GTG AG-3'

Ascl1 (sense): 5'-AGA TGA GCA AGG TGG AGA CG-3'

Ascl1 (antisense): 5'-TGG AGT AGT TGG GGG AGA TG-3'

Id1 (sense): 5'-CCC ACT GGA CCG ATC CGC CA-3'

Id1 (antisense): 5'-TGC TCT CGG TTC CCC AGG GG-3'

Table S1. Primary antibodies and dyes for immunohistochemistry

Name	Species	Company	Conc.
BrdU	Mouse monoclonal Rat monoclonal	BD Pharmingen (clone B44) Accurate Chemical & Scientific (clone BU1/75)	1:500 1:500
PECAM1	Rat monoclonal	BD Pharmingen (clone MEC13.3)	1:300
Sox2	Rabbit polyclonal Rabbit polyclonal Goat polyclonal	Stemgent #09-2024 Abcam #ab97959 Santa Cruz #sc-17320	1:500 1:1000 1:500
pHH3	Rabbit polyclonal	Upstate #07-424	1:250
cleaved caspase-3	Rabbit polyclonal	Cell Signaling #9664	1:200
S100	Rabbit polyclonal	DAKO #Z0311	1:1000
NeuN	Mouse monoclonal	Chemicon (clone A60)	1:250
Mash1	Mouse monoclonal	BD Pharmingen (clone 24B72D11.1)	1:100
Ki67	Rabbit polyclonal	Abcam #ab15580	1:300
β-catenin	Rabbit polyclonal	Sigma #C2206	1:1000
acetylated tubulin	Mouse monoclonal	Sigma (clone 6-11B-1)	1:1000
GFAP	Mouse monoclonal	Sigma (clone G-A-5)	1:1000
doublecortin	Rabbit polyclonal	Cell Signaling #4604	1:500
TO-PRO-3		Life Technologies #T3605	1:1000